Table IV. Anthracene Loss and Adduct Yield[a]

$[tt]_0$, M	degassed			stilbene			
	f_{-A} obsd	f_{-A} calcd[b]	f_{Ad} obsd	f_{-A} obsd	f_{-A} calcd[b]	f_{Ad} obsd	f_t[c]
0.065_4	0.50	0.45	0.019				
0.087_2	0.60	0.52	0.034				
0.130_8	0.66	0.54	0.040	0.74	0.58	0.029	0.35
0.174_4	0.74	0.58	0.047	0.84	0.65	0.070	0.52
0.26_3	0.84	0.65	0.10_5	0.92	0.66	0.080	0.48
0.43_6	0.96_7	0.66	0.21_7	0.98	0.72	0.20	0.47
0.61_6				0.97_9	0.73	0.27	0.41
0.87_2	0.97_1	0.73	0.31	0.97_2	0.67	0.24	0.22
1.30_8	0.97_5	0.70	0.31	0.97_3	0.68	0.30	0.19

[a] Same samples as in Table I. [b] Calculated actual loss using eq 33. [c] Fraction of *trans*-stilbene not corrected for back reaction.

thracene conversions were in the 10.1-18.3% range (UV analyses) and were not affected by bubbling air through the solutions. Diene concentrations checked were 0, 0.0876, 0.876, and 1.74 M; $[A]_0$ was 8.3×10^{-3} M throughout.

Analytical Procedures. GLC conditions for isomeric composition determinations of the hexadienes,[28] the pentadienes,[28] and the stilbenes[10] have been described previously. Diene loss to other reactions was checked at low diene concentrations by using methylcyclohexane as internal standard; GLC conditions have been described.[28] Losses were 3.0% and 15% at $[tt]_0 = 0.065$ M and 4.0% and 9.4% at $[tt]_0 = 0.174$ M for degassed and air-saturated solutions, respectively. Diene loss was taken into account in calculating isomerization quantum yields for air-saturated solutions and neglected for degassed solutions. Following the irradiation, solution absorbances were measured directly in the ampules (Cary 14 spectrophotometer), and it was determined that sufficient anthracene remained to absorb at least 95% of the incident radiation; $\epsilon = 2.7 \times 10^3$ M^{-1} cm^{-1}. GLC analyses for diene isomer composition were carried out immediately upon opening the ampules to the air. The solutions were then concentrated and analyzed for anthracene loss f_{-A}^{obsd}, 1:1 adduct, f_{Ad}^{obsd}, and, when applicable, stilbene isomerization, f_t, ($^1/_8$ in. × 3.5 ft column packed with 5% Apiezon M on Chromosorb W; column and injector temperatures were 170 °C to avoid splitting anthracene dimer). Stilbene was used as internal standard, Table IV. Anthracene concentrations determined by GLC were corrected for anthracene loss, f_{-A}, due to (at that time unknown) thermal addition of anthracene to the major 1:1 adduct,[24d] which is extensive during sample preparation,[25]

$$f_{-A} = f_{-A}^{obsd} - [f_{-A}^{obsd} - (1 + a)f_{Ad}^{obsd}]/(2 + a) \quad (33)$$

where a is the independently determined ratio of anthracene loss contributions due to dimerization and adduct formation in the absence of the thermal reaction.[25] Anthracene loss in the presence of air was obtained by adjusting the values for degassed solutions with the ratio of anthracene loss quantum yields for degassed and air-saturated solutions.[25]

Flash-Kinetic Measurements. The apparatus and procedure used for these measurements have been described.[13]

Registry No. Anthracene, 120-12-7; (*E,E*)-2,4-hexadiene, 5194-51-4; (*E,Z*)-2,4-hexadiene, 5194-50-3; (*Z,Z*)-2,4-hexadiene, 6108-61-8; (*Z*)-stilbene, 645-49-8; (*E*)-stilbene, 103-30-0; oxygen, 7782-44-7.

Carbon-13 and Proton Two-Dimensional NMR Study of the *Ormosia* Alkaloids Panamine, Ormosanine, and Ormosinine

N. S. Bhacca,[†] M. F. Balandrin,[‡] A. D. Kinghorn,[‡] T. A. Frenkiel,[§] R. Freeman,[§] and G. A. Morris*[⊥]

Contribution from the Department of Chemistry, Louisiana State University, Baton Rouge, Louisiana 70803, the Department of Pharmacognosy and Pharmacology, University of Illinois, Chicago, Illinois 60680, the Physical Chemistry Laboratory, South Parks Road, Oxford OX1 3QZ, England, and the Department of Chemistry, University of Manchester, Manchester M13 9PL, England. *Received September 13, 1982*

Abstract: Three different types of two-dimensional NMR spectroscopy have been used to study the *Ormosia* alkaloids panamine, ormosanine, and ormosinine. By assigning the proton and carbon-13 NMR spectra of panamine and ormosanine, it has proved possible to establish the previously unknown structure of ormosinine as a molecule of panamine linked at C21 to C22 of ormosanine.

Introduction

Although *Ormosia* alkaloids do not have commercial utility in modern pharmacology, recent biological screening studies[1,2] suggesting sedative, hypnotic, and analgesic properties prompted our medicinal and structural examination of some of the substances in the series. The *Ormosia* alkaloids[3] ($C_{20}H_{31-35}N_3$) are pentacyclic and hexacyclic molecules that do not contain any functional groups other than the three basic ring nitrogen atoms. Because of this unusual molecular arrangement, prior to our current NMR study, detailed mapping of these compounds was limited to X-ray diffraction[5] and total synthesis.[3,6] This was how the structures of panamine $C_{20}H_{33}N_3$ (I) and ormosanine $C_{20}H_{35}N_3$ (II) were established[3,56]. However the identity of the dimer ormosinine[3,4] (III) remained in doubt; it shows a parent ion $C_{40}H_{66}N_6^+$ in its mass spectrum and sublimes to pure panamine. This paper elucidates the structure of ormosinine (III) and develops a methodology suitable for determining the structure of other *Ormosia* alkaloids. Proton and carbon-13 NMR spectroscopy is used together with the newly developed techniques of two-dimensional

[†] Louisiana State University.
[‡] University of Illinois.
[§] Physical Chemistry Laboratory, Oxford University.
[⊥] University of Manchester.

(1) Arthur, H. R.; Loos, S. N. *Aust. J. Chem.* **1967**, *20*, 809.
(2) Moran, N. C.; Quinn, G. P.; Butler, W. M. *J. Pharmacol. Exp. Ther.* **1959**, *125*, 85.
(3) Valenta, Z.; Liu, H. J. "International Review of Science, Organic Chemistry"; Wiesner, K., Ed.; Butterworths: London, 1976; Series Two, Vol. 9.
(4) Deslongchamps, P.; Valenta, Z.; Wilson, J. S. *Can. J. Chem.* **1966**, *44*, 2539-2551.
(5) Karle, I. L.; Karle, J. *Tetrahedron Lett.* **1966**, 1659-1661.
(6) (a) Naegeli, P.; Wildman, W. C.; Lloyd, H. A. *Tetrahedron Lett.* **1963**, 2069-2073. (b) Liu, H. J.; Valenta, Z.; Yu, T. T. J. *J. Chem. Soc., Chem. Commun.* **1970**, 1116. (c) Liu, H. J.; Sato, Y.; Valenta, Z.; Wilson, J. S.; Yu, T. T. J. *Can. J. Chem.* **1976**, *54*, 97-107.

0002-7863/83/1505-2538$01.50/0

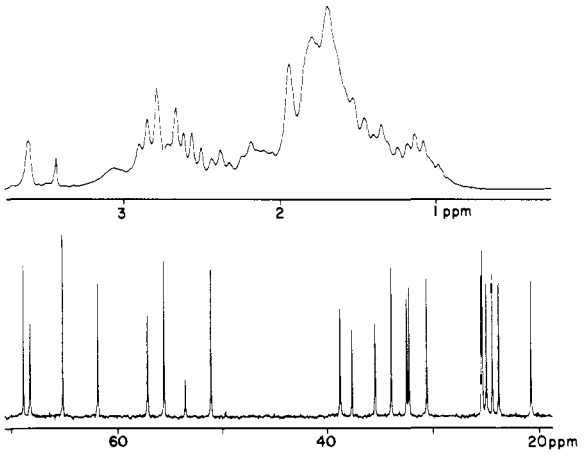

Figure 1. Proton spectrum (200 MHz) and carbon-13 spectrum (50 MHz) of panamine (I).

Fourier transformation, utilizing panamine and ormosanine as model compounds.

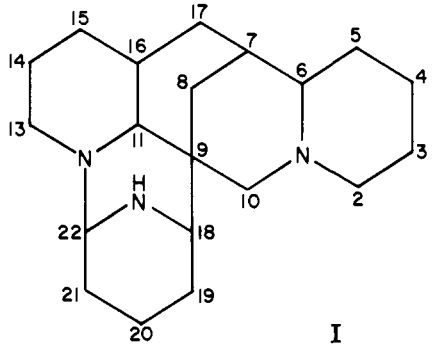

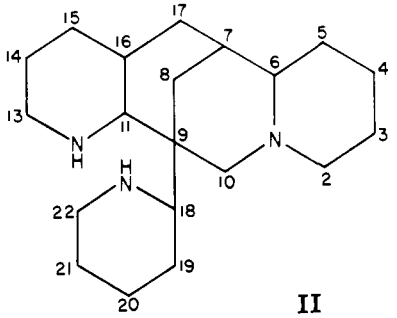

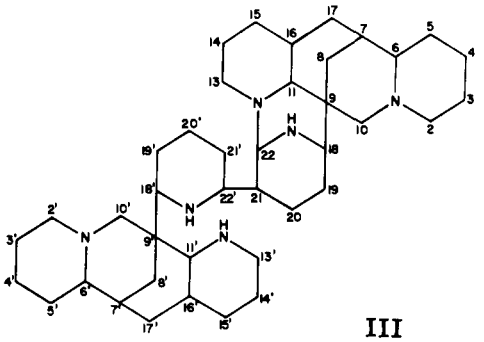

The conventional NMR spectra of protons (200 MHz) and carbon-13 (50 MHz) in compounds I–III are shown in Figures 1–3. The proton spectra remain largely unresolved and are therefore of little value, while the decoupled carbon-13 spectra have well-resolved resonances that could not be assigned because of the unavailability of spectral data on model systems. This was why two-dimensional Fourier transform spectroscopy[7-12] was

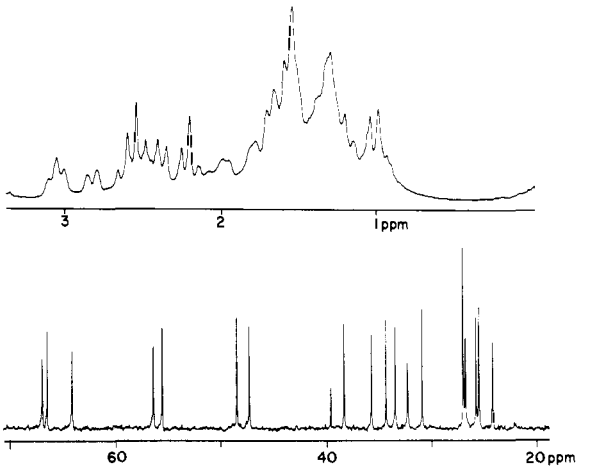

Figure 2. Proton spectrum (200 MHz) and carbon-13 spectrum (50 MHz) of ormosanine (II).

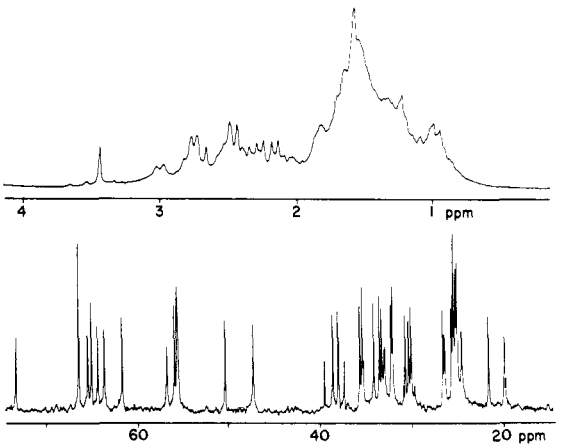

Figure 3. Proton spectrum (200 MHz) and carbon-13 spectrum (50 MHz) of ormosinine (III).

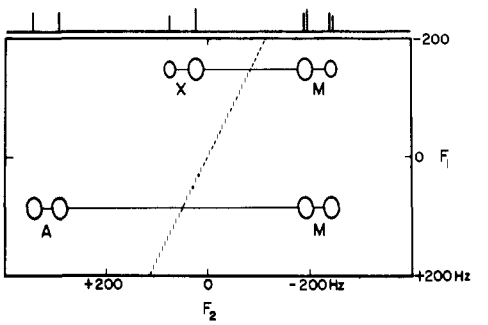

Figure 4. Model two-dimensional spectrum illustrating the carbon–carbon connectivity experiment on the fragment C_A–C_M–C_X. Direct coupling between carbon-13 spins gives rise to four-line AB or AX patterns indicated by the horizontal bars. The F_1 ordinate represents the frequency of the double-quantum coherence, equal to the sum of the appropriate carbon-13 shifts.

employed. Instead of examining the free induction decay $S(t_2)$ after a single radiofrequency pulse, this experiment introduces a new variable, the evolution time t_1 during which a series of pulses is imposed on the nuclear spin system, and t_1 is incremented in

(7) Aue, W. P.; Bartholdi, E.; Ernst, R. R. *J. Chem. Phys.* **1976**, *64*, 2229–2246.

(8) Freeman, R.; Morris, G. A. *Bull. Magn. Reson.* **1979**, *1*, 5–26.
(9) Freeman, R. *Proc. R. Soc. London, Ser. A* **1980**, *A373*, 149–178.
(10) Nagayama, K. *Adv. Biophys.* **1981**, *14*, 139–204.
(11) Morris, G. A. In "Fourier, Hadamard and Hilbert Transforms in Chemistry"; Marshall, A. G., Ed.; Plenum Press: New York, 1982.
(12) Bax, A. Ph.D. Thesis, Delft University of Technology, 1981. Bax, A. "Two-Dimensional Nuclear Magnetic Resonance in Liquids"; Reidel Publishing: Boston, 1982.

a set of successive measurements. The behavior of the nuclei during t_1 is governed by the choice of pulse sequence, and although the spectrometer receiver is not active during t_1, information about the evolution is passed on to the detected signal $S(t_2)$. This *correlation* between the behavior of a given signal during t_1 and t_2 is one of the most important properties of two-dimensional NMR spectroscopy, allowing (for example) a proton shift to be related to the corresponding carbon shift of a given site. A data matrix $S(t_1,t_2)$ is built up, stored on a disk, and subjected to two stages of Fourier transformation to give a two-dimensional spectrum, $S(F_1,F_2)$. For our structural studies of the *Ormosia* alkaloids, three different two-dimensional NMR methods were used.

Carbon–Carbon Connectivity

This is a method[13-16] for building up the connectivity of the carbon framework of the molecule one bond at a time, based on observation of the direct C–C couplings, distinguished from long-range couplings because of their size. In natural-abundance material this involves detection of the weak carbon-13 satellites of the carbon-13 spectrum, simple AX or AB patterns flanking the strong resonances from molecules containing just a single carbon-13 spin. The satellite spectrum is made much more accessible by suppressing the strong central resonances, making use of the fact that only the coupled spin systems may generate double-quantum coherence, which may be separated from single-quantum coherence because of its characteristic phase properties. After this filtration process the F_2 dimension consists of a clean spectrum of the satellites that carry the C–C coupling information.

If each coupling can be assigned unambiguously, the required connectivity information may then be deduced directly. Unfortunately this is not usually the case in practice there may be as many as four splittings of a given carbon-13 resonance, they tend to be very similar in magnitude, and they are not quite centered on the carbon chemical shift frequency because the spectra have some AB character. Unequivocal assignment requires additional information. This is provided by the frequency of the double-quantum coherence, since this is given simply by the sum of the chemical shifts of the two sites in question, measured with respect to the frequency of the carbon transmitter. Double-quantum coherence cannot be detected directly in the spectrometer, but if it is allowed to precess freely during the evolution period of a two-dimensional experiment and then converted into observable single-quantum coherence, it can be measured indirectly.

The two-dimensional spectrum obtained from such a double-quantum coherence experiment is usually presented in the form of an intensity contour plot. The main features of such a spectrum are best appreciated from a simple model case of a "linear" AMX system where A is directly bound to M and M is directly bound to X. Such a spectrum is shown in Figure 4. There are two four-line patterns (joined by the horizontal bars), which when projected onto the F_2 axis, constitute the satellite spectrum (top margin). The F_1 ordinates correspond to the appropriate double-quantum frequencies, equal to the sum of the corresponding chemical shifts. Since the midpoint of each AX or AB pattern is at the mean chemical shift, these midpoints are constrained to lie on the dotted diagonal which has $\Delta F_1/\Delta F_2 = 2$.

Since this double-quantum technique detects only signals from molecules containing two carbon-13 spins at adjacent sites, it is inherently insensitive and is only applicable when reasonably large samples are available. Typically, an acceptable two-dimensional spectrum can be obtained at 50 MHz in an overnight run if the concentration is 0.5 M. Since a 1.2 M solution (950 mg) of panamine was available, the connectivity of its carbon skeleton was established by this method. However, only 90 mg of II and 80 mg of III were available, which was insufficient for this double-quantum technique to be applied.

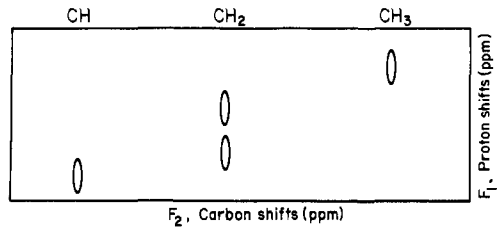

Figure 5. Model two-dimensional spectrum illustrating the proton–carbon shift correlation experiment for the molecule CH_3CH_2CHXY. Each directly bound CH group gives a resonance peak with the carbon-13 shift as abscissa and proton shift as the ordinate. The chemically nonequivalent methylene protons show two proton peaks. Proton–proton splittings are neglected in this diagram; they are usually not resolved.

Proton–Carbon Shift Correlation

This two-dimensional Fourier transform technique[17-25] identifies the resonances in the proton and carbon-13 spectra that arise from the same CH site, the criterion for correlation being that there is a large (direct) CH coupling. (The much smaller long-range couplings normally give rise to negligible responses in the two-dimensional spectrum.) Each individual proton resonance is first "labeled" by allowing it to precess at its characteristic chemical shift frequency during the evolution period t_1; this magnetization is then abruptly transferred to carbon-13 via the single-bond CH coupling. Free precession ensues during the detection period t_2 at the corresponding carbon-13 chemical shift frequency. Initially there is no net transfer because the process is only a population rearrangement, the "new" carbon-13 signals having positive and negative intensities with an algebraic sum of zero. These may be represented by pairs of vectors pointing in opposite directions, and if they are allowed a further fixed interval τ of precession while coupled to protons, with $\tau = 1/(2J_{CH})$, they come into alignment and a strong signal is observed. The trick is to choose a relatively short value of τ such that only direct couplings are large enough to give an observable signal, the vector pairs associated with long-range couplings remaining close to the antiparallel situation.

The result is a two-dimensional spectrum (often presented as an intensity contour map) where the F_1 ordinate is the proton chemical shift and the F_2 abscissa is the correlated carbon-13 shift. There are no CH splittings in either dimension, and although the usual HH splittings exist in the F_1 dimension, in practice the fine digital resolution needed to observe them is usually sacrificed in the interest of speed. This shift correlation experiment benefits from relatively high sensitivity, for although it involves the observation of natural-abundance carbon-13 signals, there is an appreciable enhancement due to transfer of proton magnetization.

Figure 5 shows a model shift correlation spectrum for a CH_3CH_2CHXY system; note that two different chemical shifts can be measured for the chemically nonequivalent methylene protons.

(13) Bax, A.; Freeman, R.; Kempsell, S. P. *J. Am. Chem. Soc.* **1980**, *102*, 4849–4851.
(14) Bax, A.; Freeman, R.; Kempsell, S. P. *J. Magn. Reson.* **1980**, *41*, 349–353.
(15) Bax, A.; Freeman, R.; Frenkiel, T. A. *J. Am. Chem. Soc.* **1981**, *103*, 2102–2104.
(16) Bax, A.; Freeman, R.; Frenkiel, T. A.; Levitt, M. H. *J. Magn. Reson.* **1981**, *43*, 478–483.
(17) Maudsley, A. A.; Ernst, R. R. *Chem. Phys. Lett.* **1977**, *50*, 368–372.
(18) Maudsley, A. A.; Müller, L.; Ernst, R. R. *J. Magn. Reson.* **1977**, *28*, 463–469.
(19) Bodenhausen, G.; Freeman, R. *J. Magn. Res.* **1977**, *28*, 471–476.
(20) Bodenhausen, G.; Freeman, R. *J. Am. Chem. Soc.* **1978**, *100*, 320–321.
(21) Freeman, R.; Morris, G. A. *J. Chem. Soc., Chem. Commun.* **1978**, 684–686.
(22) Müller, L.; Ernst, R. R. *Mol. Phys.* **1979**, *38*, 963–992.
(23) Hall, L. D.; Morris, G. A.; Sukumar, S. *J. Am. Chem. Soc.* **1980**, *102*, 1745–1747.
(24) Bax, A.; Morris, G. A. *J. Magn. Reson.* **1981**, *42*, 501–505.
(25) Morris, G. A.; Hall, L. D. *J. Am. Chem. Soc.* **1981**, *103*, 4703–4711.

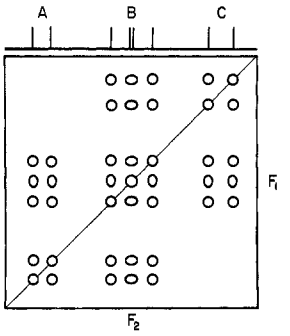

Figure 6. Model two-dimensional spectrum illustrating the proton–proton shift correlation experiment for an ABC system where J_{AC} is not resolved. Peaks on (or near) the diagonal arise from magnetization which remains associated with a given proton throughout the experiment. In contrast, the cross-peaks that lie off the diagonal arise from magnetization that is transferred from one proton to another.

Proton–Proton Shift Correlation

This is a two-dimensional experiment[26-30] that examines a many-line proton spectrum and identifies pairs of resonances that are coupled together, just as if an entire series of double-resonance experiments had been carried out. Historically this was the first two-dimensional experiment to be undertaken, and has been analyzed and extensively developed by Ernst and co-workers.[7] As in the heteronuclear correlation experiments described above, this technique relies on magnetization transfer via the spin–spin coupling, but for protons there is no division into the two classes of large and small couplings. The technical aspects of this experiment have been analyzed in detail by Bax.[12] Since protons precess freely during both the evolution and detection periods, there is a symmetry between the two frequency dimensions. The conventional proton spectrum appears along the principal diagonal ($F_1 = F_2$) and can be thought of as originating in magnetization that remains associated with a given proton during both t_1 and t_2. Magnetization transfer from one proton A to another proton X gives rise to cross-peaks that always lie off the principal diagonal, having coordinates determined by the chemical shifts of A and X. Since transfer may occur in both directions (A to X or X to A), there are two such cross-peaks symmetrically placed with respect to the principal diagonal. Each cross-peak has multiplet structure in both dimensions as illustrated in Figure 6 for a model spectrum appropriate to the "linear" ABC system of protons where the coupling between A and C is not resolved.

The lines within a multiplet are always made up of pairs with equal positive and negative intensities. For a simple AX system, the component lines of a given pair are separated by J hertz, so that if the coupling constant is very small ($JT_2 \ll 1$), the two lines are not resolved, the antiphase intensities cancel, and no cross-peaks are detected. A maximum cross-peak intensity is observed[12] when $t_1 = t_2 = 1/(4J)$, a property that can be exploited to emphasize couplings of a given magnitude while attenuating the effect of others. This flexibility turns out to be useful for spectra that are so complicated that a single proton–proton correlation experiment is not able to disentangle the coupling network.

Panamine (I)

The molecular framework of panamine was confirmed by carbon–carbon connectivity information deduced from Figure 7. For example, it is a simple matter to identify the quaternary carbon C9 because of its long spin–lattice relaxation time; this provides a good starting point for tracing the carbon–carbon linkages along four distinct paths (each of which may branch) terminating at low-field carbon sites directly bound to nitrogen atoms (C11, C22, C6, C10, C18, C2, and C13). This information is complemented by recording the carbon-13–proton two-dimensional J spectrum,[8] which gives the number of directly attached protons at each carbon site. This step-by-step construction of the carbon skeleton permits an unambiguous assignment and leads to a direct elucidation of the structure without the need for information on model compounds or the usual decisions based on substituent effects on chemical shifts. However, the double-quantum experiment requires strong solutions in order to obtain an acceptable signal-to-noise ratio.

The proton–carbon shift correlation spectrum (Figure 8) then gives the proton shift(s) for each carbon-13 resonance, thus assigning the proton spectrum of panamine.

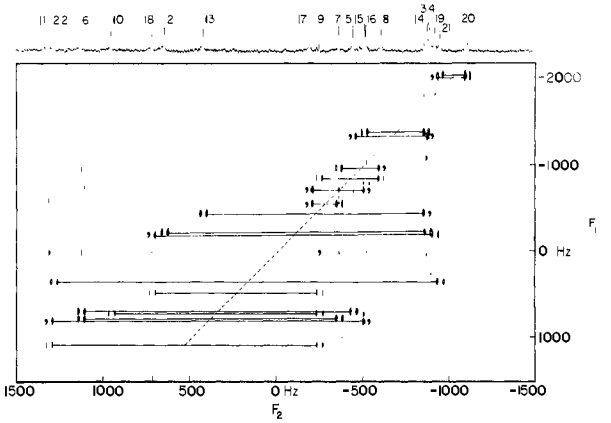

Figure 7. Carbon–carbon connectivity spectrum of panamine (I). The conventional (decoupled) spectrum runs along the top margin. Horizontal bars emphasize the AB or AX subspectra from directly coupled pairs of carbon-13 spins. The midpoints of these subspectra lie on the dotted diagonal. The F_1 ordinates are the double-quantum frequencies.

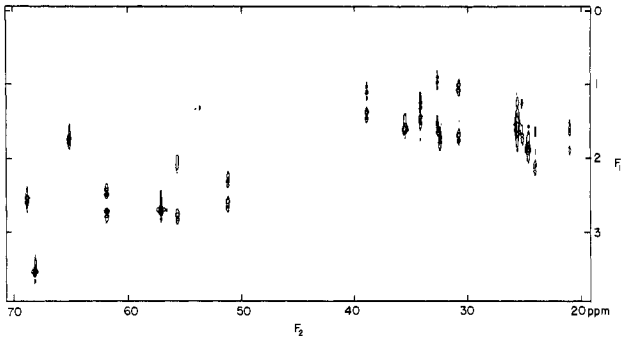

Figure 8. Proton–carbon shift correlation spectrum of panamine (I). The proton shifts are the F_1 ordinates and the carbon-13 shifts are the F_2 abscissae. Several examples of chemically nonequivalent methylene protons are evident.

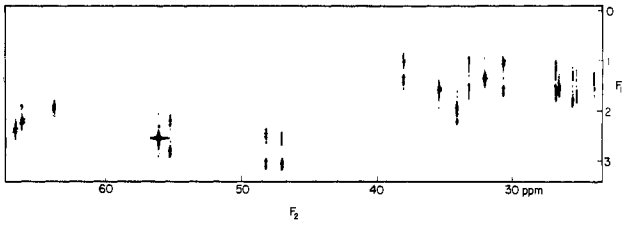

Figure 9. Proton–carbon shift correlation spectrum of ormosanine (II).

Ormosanine (II)

The small quantity of ormosanine available precluded a carbon–carbon connectivity experiment, so the first step toward the assignment was to record the proton–carbon shift correlation spectrum (Figure 9). It is often useful to replot such results in the form of a schematic map,[25] since this allows two different spectra to be compared in detail, for example, by using one in the

(26) Jeener, J. Ampere International Summer School, Basko Polje, Yugoslavia, 1971.
(27) Nagayama, K.; Wüthrich, K.; Ernst, R. R. *Biochem. Biophys. Res. Commun.* **1979**, *90*, 305–311.
(28) Nagayama, K.; Kumar, A.; Wüthrich, K.; Ernst, R. R. *J. Magn. Reson.* **1980**, *40*, 321–334.
(29) Kumar, A.; Wagner, G.; Ernst, R. R.; Wüthrich, K. *Biochem. Biophys. Res. Commun.* **1980**, *96*, 1156–1163.
(30) Bax, A.; Freeman, R.; Morris, G. A. *J. Magn. Reson.* **1981**, *42*, 164–168.

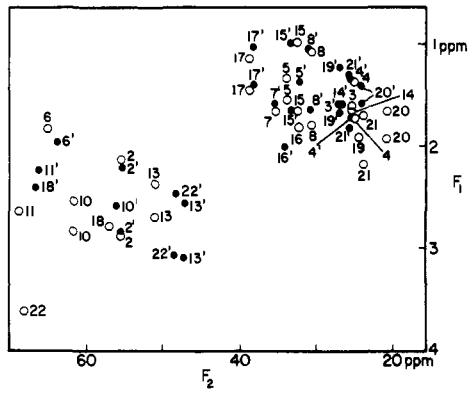

Figure 10. Map obtained by replotting the proton–carbon shift correlation data of panamine (open circles) and ormosanine (black circles) with an indication of the assignments.

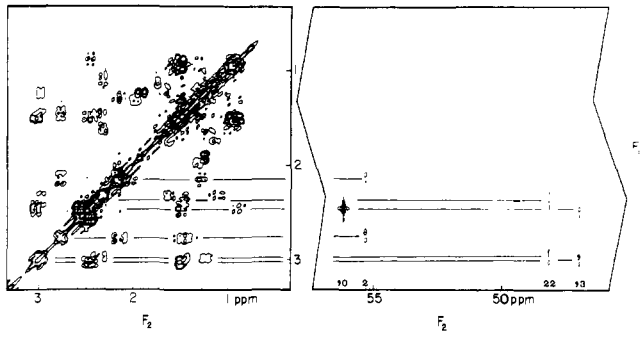

Figure 11. Proton–proton (left) and proton–carbon (right) shift correlation spectra of ormosanine (II) obtained under identical experimental conditions so that the two F_1 scales may be directly compared. Proton shifts from the right-hand spectrum, identified via the carbon-13 shifts, are used to disentagle the cross-peaks in the left-hand spectrum.

form of a transparent overlay. Figure 10 shows the appropriate schematic plots for panamine (open circles) and ormosanine (black circles). Comparison of these two sets of results brings out the fact that they have a common molecular framework. Together with the carbon multiplicities determined from the two-dimensional J spectra,[8] this allows the assignment of resonances 2,5–10, and 15–17.

In order to make the remaining assignments, it is necessary to investigate the coupling relationships between the protons, by using the proton shifts measured from the proton–carbon shift correlation experiment (Figure 9). Because of the overcrowding of the proton spectrum it is important that the proton–proton correlation spectrum[26-30] be measured on the same sample as the proton–carbon shift correlation spectrum and under the same conditions. This allows direct and accurate comparisons to be made between the two. Accordingly the proton–proton shift correlation spectrum of Figure 11 was measured by using the decoupler coil of the Varian XL-200 10-mm probe as the receiver coil, retaining the same proton transmitter frequency and the same spectral width as for the F_1 dimension of the proton–carbon shift correlation spectrum. The two types of shift correlation spectrum may then be compared directly, identifying individual cross-peaks in the proton–proton shift correlation spectrum with the appropriate proton shifts in the proton–carbon shift correlation spectrum even though a number of proton multiplets may be superimposed. Figure 11 illustrates this method of identification for the case of the methylene protons on C13 and C22.

The proton–proton shift correlation information was then used to assign the remaining proton (and hence carbon-13) shifts of ormosanine. Those for C11, C20, and C22 were identified by elimination since they give rise to strongly coupled multiplets with cross-peaks lying close to the principal diagonal. This is a general weakness of homonuclear correlation spectra when the coupled protons have only a small chemical shift difference; the cross-peaks tend to merge into the skirts of the stronger diagonal peaks. This

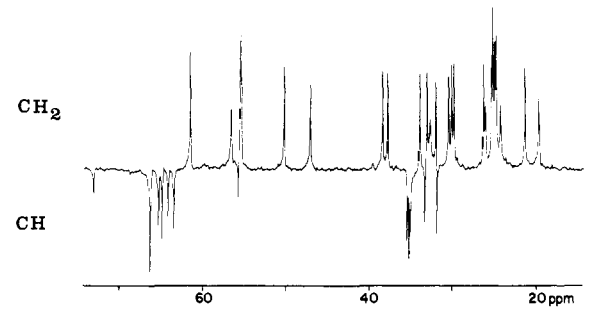

Figure 12. Multiplicities of the carbon sites in ormosinine (III) determined by means of the INEPT experiment. Quaternary resonances are suppressed, CH_2 sites give positive intensities while CH sites give negative intensities; there are no CH_3 groups in this molecule.

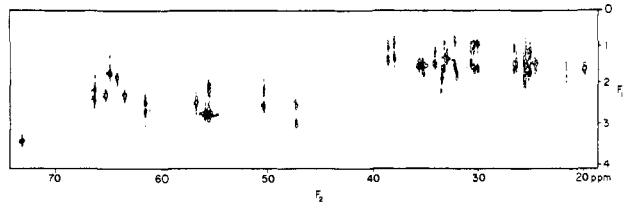

Figure 13. Proton–carbon shift correlation spectrum from ormosinine (III).

completed the assignment of the proton and carbon-13 spectra of the two model compounds panamine (I) and ormosanine (II), summarized in Figure 10.

Ormosinine (III)

The quantity of ormosinine available for study was less even than that of ormosanine, thus ruling out the carbon–carbon experiment. The quest for higher sensitivity favored a different method of determining carbon-13 multiplicities—the INEPT experiment.[31-35] This produces a decoupled carbon-13 spectrum in which quaternary signals are suppressed, while CH_2 signals (positive intensities) are distinguished from CH_3 and CH signals (negative intensities). In practice this method worked better than off-resonance coherent decoupling or spin–lattice relaxation measurements for determining multiplicity, since it was less susceptible to overlap problems. For example, in Figure 12, the doublet C18 is just resolved from the two triplets C2 and C2′, whereas with off-resonance decoupling this assignment was ambiguous. This technique gives an excellent signal-to-noise ratio and is particularly suited to systems (such as those under study here) where all the direct CH coupling constants are within a narrow range. Since ormosinine contains no methyl groups, all the multiplicity information is obtained from a single INEPT spectrum (Figure 12).

A proton–carbon shift correlation spectrum of ormosinine is shown in Figure 13. The corresponding proton–proton shift correlation is shown in Figures 14 and 15. For these spectra the same experimental data matrix was processed in two different ways, first with a "pseudo-echo" weighting function[36] to give a line width of about 15 Hz (Figure 14) and then with a much milder weighting function (Figure 15). With the severe line broadening of Figure 14, the individual components of a cross-peak mutually cancel for all couplings less than about 10–15 Hz since they have antiphase intensities. The correlation map is thus restricted to protons with large values of J_{HH}. By contrast, Figure 15 emphasizes the correlations through small coupling constants—often longer range interactions. Examination of the two differently processed spectra allows many more correlations

(31) Morris, G. A.; Freeman, R. *J. Am. Chem. Soc.* **1979**, *101*, 760–762.
(32) Morris, G. A. *J. Am. Chem. Soc.* **1980**, *102*, 428–429.
(33) Burum, D. P.; Ernst, R. R. *J. Magn. Reson.* **1980**, *39*, 163–168.
(34) Doddrell, D. M.; Pegg, D. T. *J. Am. Chem. Soc.* **1980**, *102*, 6388–6390.
(35) Morris, G. A. *J. Magn. Reson.* **1980**, *41*, 185–188.
(36) Bax, A.; Freeman, R.; Morris, G. A. *J. Magn. Reson.* **1981**, *43*, 333–338.

Table I. Carbon-13 and Proton Chemical Shifts[a] for Panamine (I), Ormosanine (II), and Ormosinine (III)

	panamine (I)			ormosanine (II)			ormosinine (III)					
							panamine moiety			ormosanine moiety		
	carbon	protons		carbon	protons		carbon	protons		carbon	protons	
C2	55.41	2.12	2.87	55.23	2.19	2.83	55.50	2.00	2.75	55.42	2.11	2.73
C3	25.27	1.60		26.83	1.57		25.45[b]	1.51		24.57	1.43	
C4	24.94	1.31	1.72	25.29	1.34	1.71	26.59	1.08	1.55	25.21	1.18	1.60
C5	33.85	1.33	1.54	32.05	1.36		34.10	1.18	1.45	32.94	1.33	
C6	64.98	1.82		63.78	1.94		64.86	1.68		64.18	1.79	
C7	35.30	1.65		35.43	1.57		35.59[c]	1.51		35.31[c]	1.53	
C8	30.56	1.07	1.79	30.67	1.05	1.63	30.32[d]	0.98	1.51	30.05[d]	0.97	1.53
C9	37.57			39.29			37.30			39.44		
C10	61.58	2.53	2.82	56.06	2.55		61.50	2.43	2.67	56.64	2.43	
C11	68.66	2.63		66.13	2.21		65.29	2.24		66.27	2.12	
C13	50.96	2.36	2.68	46.98	2.55	3.08	50.27	2.12	2.53	47.24	2.49	2.94
C14	25.38	1.64		26.58	1.57		25.47[b]	1.51		26.39	1.47	
C15	32.42	0.98	1.65	33.21	0.98	1.64	32.22	0.89	1.48	33.25	0.92	1.53
C16	32.25	1.81		34.09	1.99		32.06	1.69		33.50	1.83	
C17	38.68	1.14	1.45	38.03	1.02	1.39	38.55	1.01	1.35	37.96	0.91	1.31
C18	56.78	2.77		66.60	2.39		55.80	2.71		66.27	2.35	
C19	24.40	1.91		26.80	1.22	1.66	25.66	1.78		30.69	1.03	1.43
C20	20.74	1.65	1.92	24.00	1.40	1.57	21.63	1.51	1.82	19.89	1.56	
C21	23.80	1.69	2.17	25.58	1.29	1.84	35.19	1.72		25.05	1.16	1.67
C22	68.00	3.61		48.15	2.45	3.07	73.09	3.42		63.43	2.25	

[a] Referred to tetramethylsilane indirectly; standard deviation 0.02 ppm. [b-d] Assignments may be interchanged.

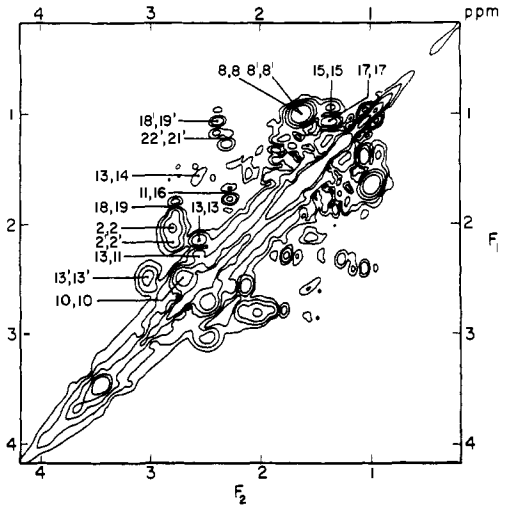

Figure 14. Proton–proton shift correlation spectrum from ormosinine (III) obtained by processing the experimental data with a severe line-broadening function in order to emphasize the large proton–proton couplings. Selected assignments are indicated, with primes denoting the ormosanine moiety.

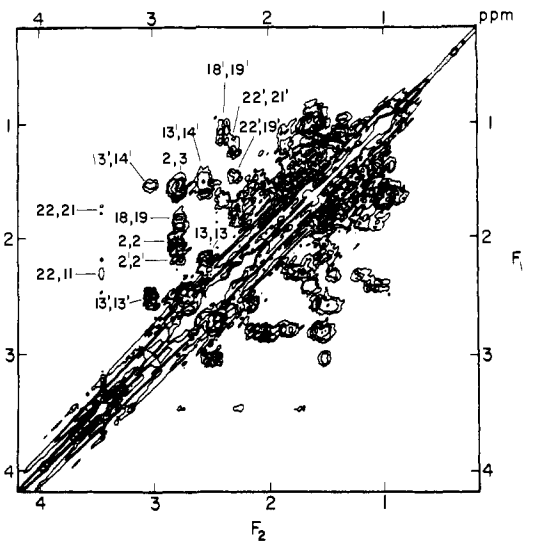

Figure 15. Same experimental data set as in Figure 14 processed with a mild line-broadening function in order to emphasize correlations through small proton–proton couplings.

to be identified than with a single spectrum having compromise weighting. It should be emphasized that it is important to suppress the broad dispersion-mode skirts of the resonances in the two-dimensional spectrum, otherwise interpretation is rendered very difficult because of overlap problems. The "pseudo-echo" weighting function accomplishes this very effectively (at the expense of a loss of sensitivity).

Comparison between the data of Figure 16 and the model compound shift map of Figure 10 suggests strongly that ormosinine (III) consists of a panamine (I) unit linked to an ormosanine (II) unit. Detailed analysis using the proton–proton couplings identified in Figures 14 and 15 confirms this, suggesting a linkage between C21 of panamine and C22 of ormosanine. This corresponds to the same skeleton as that proposed for ormojine,[37] a dimer of ormosajine, a diastereomer of panamine differing in stereochemistry at C11 and C18.[3] The assignment proceeds as follows. With use of a comparison between the ormosinine chemical shift map (Figure 16) and the model compound map (Figure 9), resonances 2, 2', 5, 5', 6, 6', 7, 7' 10, 10', 11', 13, 13', 15, 15', 16, 16', 17, 17', 18, 21, and 22 may be assigned, together with the two quaternary carbons 9 and 9'. The broadened proton–proton shift correlation spectrum of Figure 14 shows clearly the trans couplings 11–16 and 18–19, as well as the expected geminal couplings, allowing 18' and 22' to be identified by elimination. In the high-resolution spectrum (Figure 15), couplings 18'–19' and 18'–20' identify these signals, in turn assigning 8, 8', and 20 by elimination. Cross-peaks were also assigned provisionally to the couplings 2–3, 2'–3', 2–4, 2'–4', 12–14, 13–14, 13'–14', and 21'–22'; the assignments for the series 2–3–4 and 2'–3'–4' rely on the larger axial–equatorial proton shift difference for C2 in the panamine unit and could be interchanged, while the shift differences between 21' and 4' are sufficiently small for there to be a possibility of error. The only remaining ambiguities are between 8 and 8', 7 and 7', and 3 and 14, which show virtually identical shifts. None of the ambiguities affect the evidence for the proposed structure. The assigned proton and carbon-13 chemical shifts for ormosinine are listed in Table I and plotted out in Figure 16 to facilitate comparison with the model compound shifts in Figure 9. It is of interest to note that the upfield carbon-13 shift of C20' suggests very strongly a trans relationship for the linkages at C18' and C22'; unfortunately strong coupling obscures

(37) Davies, A. P.; Hassall, C. H. *Tetrahedron Lett.* **1966**, 6291–6294.

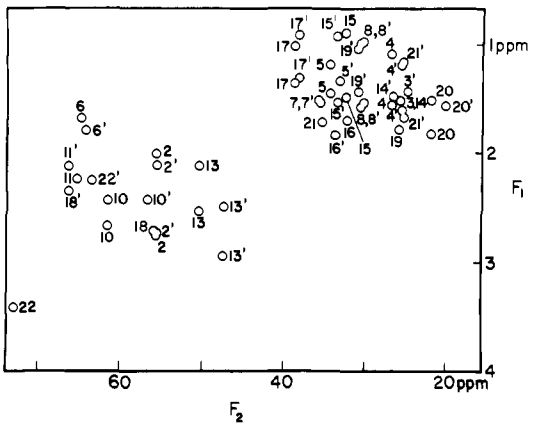

Figure 16. Map obtained by replotting the proton–carbon shift correlation results for ormosinine (III) from Figure 13, with primes denoting the ormosanine moeity. A detailed comparison with the map of Figure 10 indiates that ormosinine (III) is made up of panamine (I) and ormosanine (II).

the coupling constant H20–H21 that might indicate the configuration at the last stereochemical uncertainity, C21.

Discussion

The compounds investigated here provide illustration of two useful routes to structure elucidation and the assignment of proton and carbon-13 chemical shifts. Determination of the connectivity of the carbon skeleton[16] is a powerful but insensitive technique, requiring (at 50-MHz carbon-13 resonance) at least 0.5 M concentration but giving very detailed information about the molecular framework. The analysis of these double-quantum spectra is simple and largely unequivocal; however, in order to determine stereochemistry, it is usually necessary to turn to the proton spectrum (which is often only poorly resolved) by using proton–proton correlation spectroscopy. Proton–carbon shift correlation[24] is practicable at concentrations down to 10–20 mM on the instrument used, and with simpler spectra than those discussed here can often be used directly to assign proton and carbon-13 spectra. In very complex systems the measurement of the proton–proton correlation spectrum[28,30] not only allows the identification of individual proton resonances that would otherwise remain unresolvable but enables the structure of a molecule to be mapped out by correlations through C–H–H–C coupling relationships. Although much less direct than the double-quantum method, this route is navigable at much lower concentrations and, as seen above, can unravel very tangled spectra. It is, however, essential in such crowded spectra to ensure identical conditions for the two kinds of shift correlation experiment, since an error in registration of only a few hertz could prevent an unequivocal assignment being made.

Two-dimensional NMR is more difficult to use than conventional NMR, and the interpretation of the spectra is often as time-consuming as their measurement. Nevertheless the experiments described above can be implemented on most Fourier transform NMR spectrometers and are widely and generally applicable. When the conventional NMR spectra lie near the limits of resolving power for a particular instrument, the case for using two-dimensional NMR is a strong one.

Acknowledgment. This work was made possible by an equipment grant and a Research Studentship (T.A.F) from the Science and Engineering Research Council (U.K.) We are grateful to Dr. P. Naegeli, Givandan Research Company Ltd., Zurich, Switzerland, for samples of ormosanine, ormosinine, and panamine diperchlorate.

Registry No. Panamine, 2448-27-3; ormosanine, 5001-21-8; ormosinine, 14350-67-5.

Electrochemical Studies of the Reduction of Fluorenone Triphenylphosphazine. Formation of the Stable Dimeric Dianion, $(FlN_2)_2^{2-}$

Dale E. Herbranson, F. J. Theisen, M. Dale Hawley,* and Richard N. McDonald*

Contribution from the Department of Chemistry, Kansas State University, Manhattan, Kansas 66506. *Received November 10, 1982*

Abstract: The electrochemical reduction of fluorenone triphenylphosphazine (Fl=NN=PPh_3) in *N,N*-dimethylformamide–0.1 M $(n\text{-Bu})_4NClO_4$ is initially a one-electron process which affords the corresponding anion radical. Fl=NN=$PPh_3^{-\cdot}$ is unstable on the cyclic voltammetric time scale, decomposing by nitrogen–phosphorus bond cleavage (k = 0.45 s^{-1} at T = 1 °C) to give PPh_3 and 9-diazofluorene anion radical ($FlN_2^{-\cdot}$). The latter species then reacts rapidly with either Fl=NN=PPh_3 or $FlN_2^{-\cdot}$ to give a stable dimeric dianion. The dianion, which was shown from chronoamperometric and coulometric gas-pressure studies to have the empirical formula $(FlN_2)_2^{2-}$, is oxidized in successive one-electron steps to $(FlN_2)_2$ which slowly loses N_2 on the cyclic voltammetric time scale to give fluorenone azine (Fl=NN=Fl). The structure of the dimeric species is considered to be the tetraazatriene Fl=NN=NN=Fl. No evidence was obtained for the formation of the carbene anion radical, $Fl^{-\cdot}$, via the loss of N_2 from $FlN_2^{-\cdot}$.

Introduction

Carbenes have been prepared from several classes of organic compounds, including diazoalkanes, diazirines, oxiranes, and phosphazines.[1] Certain diazoalkanes also appear to be well-suited for the preparation of carbene anion radicals ($R_2C^{-\cdot}$). For example, dissociative electron attachment to diazomethane[2] and diazocyclopentadiene[3] in the gas phase affords methylene ($H_2C^{-\cdot}$) and cyclopentadienylidene ($c\text{-}C_5H_4^{-\cdot}$) anion radicals, respectively.

(1) (a) Jones, M., Jr.; Moss, R. A., Ed. "Carbenes"; Wiley-Interscience: New York, 1973, 1975; Vol. 1, 2. (b) Kirmse, W. "Carbene Chemistry", 2nd ed.; Academic Press: New York, 1971.

(2) Zittel, P. F.; Ellison, G. B.; O'Neil, S. V.; Lineberger, W. C.; Reinhardt, W. R. *J. Am. Chem. Soc.* **1976**, *98*, 3732.

(3) McDonald, R. N.; Chowdhury, A. K.; Setser, D. W. *J. Am. Chem. Soc.* **1980**, *102*, 6491.

0002-7863/83/1505-2544$01.50/0